

# Convergent optical wired and wireless long-reach access network using high spectral-efficient modulation

C. W. Chow\* and Y. H. Lin

Department of Photonics and Institute of Electro-Optical Engineering, National Chiao Tung University, Hsinchu 30010, Taiwan

\* cwchow@faculty.nctu.edu.tw

**Abstract:** To provide broadband services in a single and low cost perform, the convergent optical wired and wireless access network is promising. Here, we propose and demonstrate a convergent optical wired and wireless long-reach access networks based on orthogonal wavelength division multiplexing (WDM). Both the baseband signal and the radio-over-fiber (ROF) signal are multiplexed and de-multiplexed in optical domain, hence it is simple and the operation speed is not limited by the electronic bottleneck caused by the digital signal processing (DSP). Error-free demultiplexing and down-conversion can be achieved for all the signals after 60 km (long-reach) fiber transmission. The scalability of the system for higher bit-rate (60 GHz) is also simulated and discussed.

©2012 Optical Society of America

**OCIS codes:** (060.0060) Fiber optics and optical communications; (060.2360) Fiber optics links and subsystems; (350.4010) Microwaves.

---

## References and links

1. G.-K. Chang, J. Yu, Z. Jia, and J. Yu, "Novel optical-wireless access network architecture for simultaneously providing broadband wireless and wired services," Proc. OFC, Anaheim, USA, 2006, Paper OFM1D.
2. A. Chowdhury, H.-C. Chien, S. Khire, S.-H. Fan, X. Tang, N. Jayant, and G.-K. Chang, "Next-generation e-health communication infrastructure using converged super-broadband optical and wireless access system," Proc. WoWMoM, pp. 1–5, Montreal, Canada, 2010.
3. D. Qian, J. Hu, P. N. Ji, and T. Wang, "10-Gb/s OFDMA-PON for delivery of heterogeneous services," Proc. OFC, 2008, Paper OWH4.
4. B. Liu, X. Xin, L. Zhang, K. Zhao, and C. Yu, "Broad convergence of 32QAM-OFDM ROF and WDM-OFDM-PON system using an integrated modulator for bidirectional access networks," Proc. OFC, 2010, Paper JThA26.
5. C. W. Chow, C. H. Yeh, C. H. Wang, F. Y. Shih, and S. Chi, "Signal remodulated wired/wireless access using reflective semiconductor optical amplifier with wireless signal broadcast," IEEE Photon. Technol. Lett. **21**(19), 1459–1462 (2009).
6. C. W. Chow, C. H. Yeh, L. Xu, and H. K. Tsang, "Rayleigh backscattering mitigation using wavelength splitting for heterogeneous optical wired and wireless access networks," IEEE Photon. Technol. Lett. **22**(17), 1294–1296 (2010).
7. Y. Y. Won, H. S. Kim, Y. H. Son, and S. K. Han, "Network supporting simultaneous transmission of millimeter-wave band and baseband gigabit signals by sideband routing," J. Lightwave Technol. **28**(16), 2213–2218 (2010).
8. K. Ikeda, T. Kuri, and K. Kitayama, "Simultaneous three-band modulation and fiber-optic transmission of 2.5-Gb/s baseband, microwave-, and 60-GHz-band signals on a single wavelength," J. Lightwave Technol. **21**(12), 3194–3202 (2003).
9. M. Bakaul, A. Nirmalathas, C. Lim, D. Novak, and R. Waterhouse, "Hybrid multiplexing of multiband optical access technologies towards an integrated DWDM network," IEEE Photon. Technol. Lett. **18**(21), 2311–2313 (2006).
10. C. Lim, A. Nirmalathas, D. Novak, R. Waterhouse, and G. Yoffe, "Millimeter-wave broadband fiber-wireless system incorporating baseband data transmission over fiber and remote LO delivery," J. Lightwave Technol. **18**(10), 1355–1363 (2000).
11. W. Shieh and C. Athaudage, "Coherent optical orthogonal frequency division multiplexing," Electron. Lett. **42**(10), 587–588 (2006).
12. A. D. Ellis and F. C. G. Gunning, "Spectral density enhancement using coherent WDM," IEEE Photon. Technol. Lett. **17**(2), 504–506 (2005).
13. G. Goldfarb, G. Li, and M. G. Taylor, "Orthogonal wavelength-division multiplexing using coherent detection," IEEE Photon. Technol. Lett. **19**(24), 2015–2017 (2007).
14. D. B. Payne and R. P. Davey, "The future of fiber access systems," BT Technol. J. **20**(4), 104–114 (2002).

15. C. W. Chow, C. H. Yeh, C. H. Wang, F. Y. Shih, C. L. Pan, and S. Chi, "WDM extended reach passive optical networks using OFDM-QAM," *Opt. Express* **16**(16), 12096–12101 (2008).
  16. A. Stöhr, A. Akrouf, R. Buß, B. Charbonnier, F. van Dijk, A. Enard, S. Fedderwitz, D. Jäger, M. Huchard, F. Lecoche, J. Marti, R. Sambaraju, A. Steffan, A. Umbach, and M. Weiß, "60 GHz radio-over-fiber technologies for broadband wireless services [Invited]," *J. Opt. Netw.* **8**(5), 471–487 (2009).
- 

## 1. Introduction

Future access networks need to provide broadband services using wired and wireless approaches. The convergent optical wired and wireless access network has been proposed to provide broadband services in a single and integrated perform. Passive optical network (PON) is promising for providing wired services, while radio-over-fiber (ROF) is an important technique for providing wireless services in the optical domain. The simultaneous generation and transmission of both signals for PON and ROF for the convergent optical wired and wireless has been proposed and demonstrated [1–10]. The scheme reported in [8] only needs a single electro-absorption modulator (EAM) to produce baseband and ROF signal simultaneously. However, the signal performance is limited by the nonlinearity, chirp of the EAM. Techniques used in the integrated ROF and access networks reported in [6] and [9] either require optical modulator at the remote node (RN) or multiple laser sources. These will complicate the system. System reported in [10] requires electrical up-conversion at each base station, which is costly and complicated. Techniques used in [1] and [7] can provide simple generation and demodulation of the baseband and ROF signal, however, the frequency separation between the two bands signal should be larger than the bandwidth of the signal to avoid cross-talk. Our proposed convergent optical wired and wireless scheme is spectral efficient, in which the channel spacing equals the bit-rate per subcarrier. It does not require multiple laser sources, or electrical up-conversion at the RN or at the base station.

Recently, using orthogonal multi-carrier modulations provide cost-effective and high spectral-efficient optical communication. These modulations include orthogonal frequency division multiplexing (OFDM) [11], coherent wavelength division multiplexing (WDM) [12] and orthogonal WDM [13]. And orthogonal WDM is promising since its operation speed does not limited by the electronic bottleneck caused by the digital signal processing (DSP). Besides, long-reach (LR) access can integrate the metro and access for simplifying the network architecture [14]. In this work, we propose and demonstrate a convergent optical wired and wireless LR access networks based on orthogonal WDM. High signal spectral-efficiency can be obtained. Although spectral efficiency is not the top priority issue for the present access networks, it is not true for the case of WDM LR access (since it integrate the present metro and access sections [14, 15]). As the optical amplifier has a fixed and limited bandwidth of about 30 nm. Increasing the spectral efficiency of the WDM LR access is essential. Here 5 Gb/s baseband non-return-to-zero (NRZ) signal and 10 GHz double sideband ROF signal (carrying 5 Gb/s data) are orthogonally wavelength-division-multiplexed. They occupy a bandwidth of 20 GHz. Error-free de-multiplexing and down-conversion can be achieved after 60 km (long-reach) of single-mode fiber (SMF) transmission without dispersion compensation. Time-delays and power differences between the baseband NRZ and the ROF signals in the transmitter (Tx) are characterized. The scalability of the system for higher bit-rate (60 GHz) is also discussed.

## 2. Experiment of the convergent long-reach optical wired and wireless access

Figure 1 shows the experimental setup of the wired and wireless access network. A continuous wave (CW) signal at wavelength of 1550.97 nm was divided into two paths by a 3-dB coupler. A Mach-Zehnder modulator (MZM<sub>1</sub>) at the upper path was used to produce a 5 Gb/s, pseudorandom binary sequence (PRBS)  $2^{31}-1$  baseband NRZ signal for optical wired application. In the lower path, two coherent optical tones of 10 GHz apart were first generated by the MZM<sub>2</sub>, which was dc-based at the transmission null and was electrically driven by a 5 GHz clock. The optical two tones were then launched into MZM<sub>3</sub> to produce the double sideband carrier suppressed ROF signal (10 GHz sinusoidal signal carrying 5 Gb/s NRZ signal). Time-delay and power differences between the baseband NRZ signal and the ROF

signal were adjusted by using electrical delay-line and variable optical attenuator (VOA) respectively. They will be discussed in section 4. An erbium-doped fiber amplifier (EDFA) was used in the remote node (RN) to provide an output saturation power of 23 dB. Optical amplifiers are usually included in LR-PON [14, 15]. Here, the EDFA was used to compensate the power loss of the 60 km SMF and the 1:32 fiber splitter. Then a passive optical delay interferometer (DI) of 100 ps was used as an optical filter and optical de-multiplexer to demultiplex the baseband and the ROF signal. The 100 ps DI provides the free spectral range (FSR) of 10 GHz; hence allowing the ROF signal to pass through at one of the output port ( $f_0 \pm 5$  GHz), and allowing the baseband NRZ signal to pass through at the other output port ( $f_0$ ) as shown in Fig. 1. At the receiver (Rx), the baseband signal was directly detected by a photodiode (PD<sub>1</sub>) (5 GHz bandwidth) for PON application. Then, the ROF signal was launched into PD<sub>2</sub> (20 GHz bandwidth). The self-beating of the NRZ signal will produce the baseband signal while the coherent beating between the two optical tones (two sidebands) will produce the radio-frequency (RF) signal at 10 GHz frequency band. An electrical diplexer was used to separate the baseband-detected ROF signal and the RF signal. The RF signal can then be directly emitted via an antenna. In the measurement, the RF output of the diplexer was directly connected to an RF mixer for signal down-conversion. The gray boxes and yellow boxes in Fig. 1 show the schematic optical and RF spectra at different locations of the network respectively. Bit-error rate (BER) measurements were performed. Simulations using VPI Transmission Maker V7.5 were performed to confirm the experimental results.

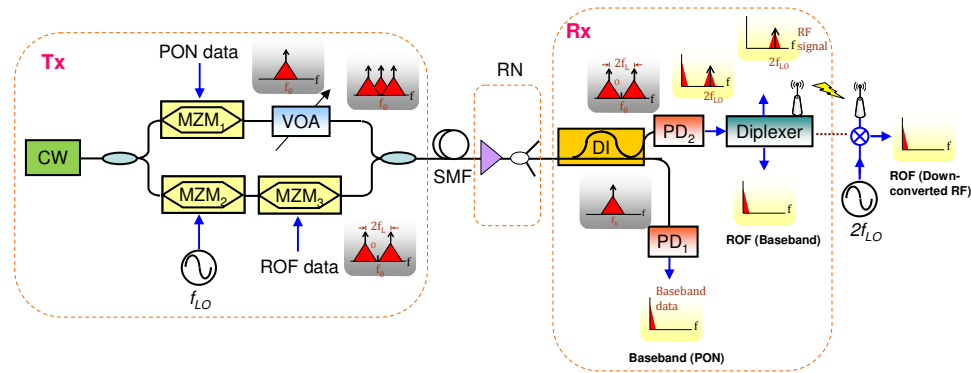


Fig. 1. Experimental setup of the convergent optical wired and wireless access network. Inset: gray box: optical spectra, yellow box: electrical spectra.

### 3. Principle of the orthogonal WDM for baseband and ROF signals

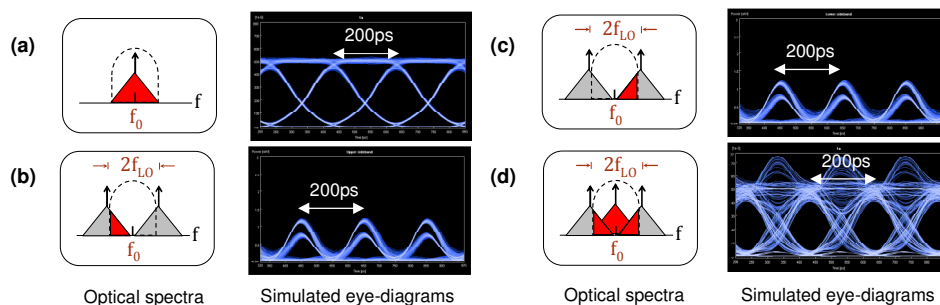


Fig. 2. Principle of orthogonal WDM for baseband and ROF signals.

In the conventional WDM, if the channel separation is not large enough, crosstalk produced by adjacent channels will highly degrade the target channel. Figure 2 shows the schematic optical spectra and simulated eye-diagrams (using VPI) for illustrating the operation principle of the proposed scheme. In our proposed scheme, high spectral-efficiency

(channel spacing is equal to the bit-rate) can be achieved by using proper time-delay. Considering the target wavelength channel at  $f_0$  (Fig. 2(a)) after passing through an optical filter (filter pass-band: dotted line), residual crosstalk from the high frequency components of the two adjacent channels will also be inside the pass-band of the optical filter, as shown in Fig. 2(b) and 2(c). The corresponding eye-diagrams are return-to-zero (RZ) liked due to the transient components of the signal in time-domain. By proper time-adjusting these transients to the eye-crossing of the target channel, clear eye-opening can be achieved

#### 4. Results and discussion

Figure 3(a) shows the BER measurements of the 5 Gb/s baseband NRZ signal for PON applications. The corresponding experimental (upper graph) and simulation eye-diagrams (lower graph) are also included in the insets. About 1 dB power penalty was observed after the long-reach 60 km SMF transmission. Figure 3(b) shows the BER measurements of the baseband-detected ROF and the down-converted ROF signal for wireless applications. About 2 dB power penalty was observed after the fiber transmission. It is observed that there is a good match between the experimental and simulation eye-diagrams. It is also observed that although there is a large spectral overlap between the baseband wired signal and the ROF signal (as described in section 2 above), by adjusting the proper time-delay, error-free demultiplexing and signal detection can be achieved after the long-reach transmission. Figure 4 shows the experimental optical spectra (using optical spectrum analyzer with resolution of 0.01 nm) measured respectively at the DI constructive and destructive output ports. We can observe that the baseband and the ROF signal can be successfully de-multiplexed by the DI.

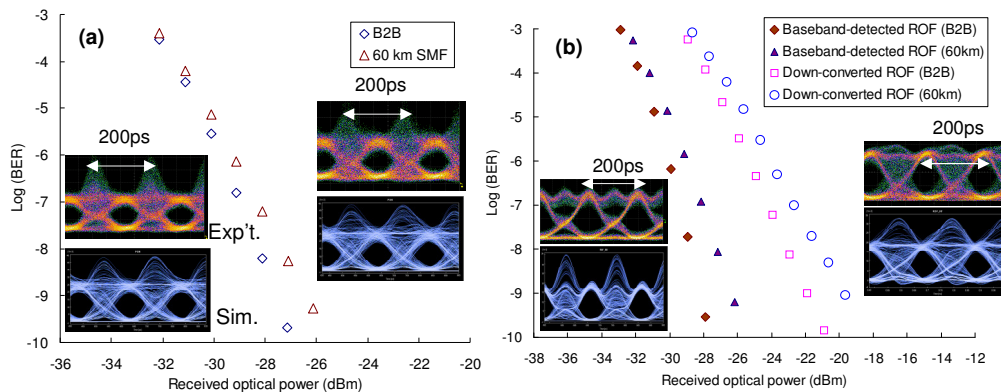


Fig. 3. BER measurements of the (a) baseband NRZ signal for PON applications and (b) baseband-detected ROF and down-converted ROF signal. Insets: corresponding experimental and simulation eye-diagrams.

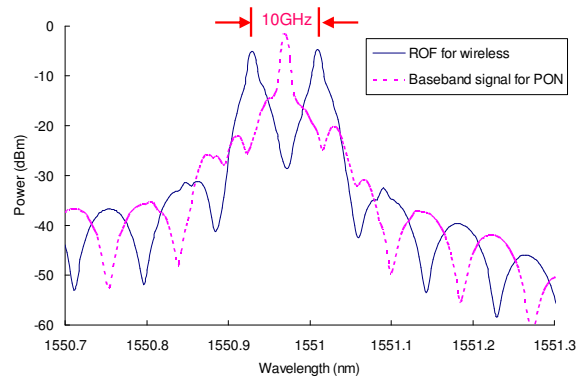


Fig. 4. Experimental optical spectra measured at constructive and destructive output ports of the DI.

Figures 5(a) and 5(b) show the experimental and simulation RF spectra measured after PD<sub>2</sub> and prior the diplexer (point 'A' in Fig. 1). We can clearly observe the baseband and RF signals in the RF spectrum. The baseband component is generated by the self-beating of the NRZ signal, and the RF signal at 10 GHz frequency band is generated by the coherent beating between the two optical tones (two sidebands). There is a good match between them.

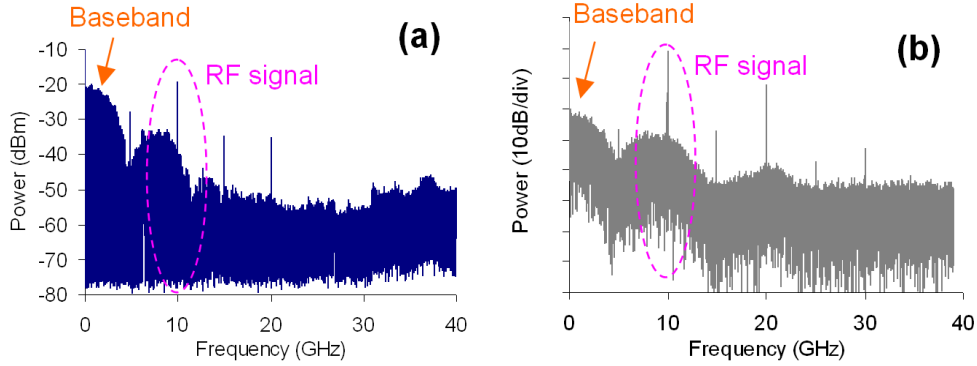


Fig. 5. (a) Measured and (b) simulated RF spectra measured after PD<sub>2</sub>.

Then we analyzed the optimum time-delay and power difference between the baseband NRZ signal and the ROF signal. Figure 6 shows the simulated Q-value of the baseband NRZ and ROF signals at different time-delays between them. As discussed in section 2, the optimum delay will happen simultaneously for both baseband NRZ and ROF signal. We can observe from Fig. 6 that the time-delay tolerance to achieve error-free operation ( $Q > 15$  dB) is quite large, and it is about 35% of a bit period. Hence, less accurate delay line can be used.

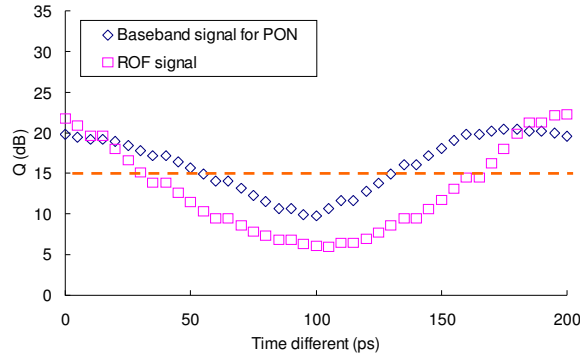


Fig. 6. Stimulated Q-value against time-delays between the baseband NRZ signal and the ROF signal.

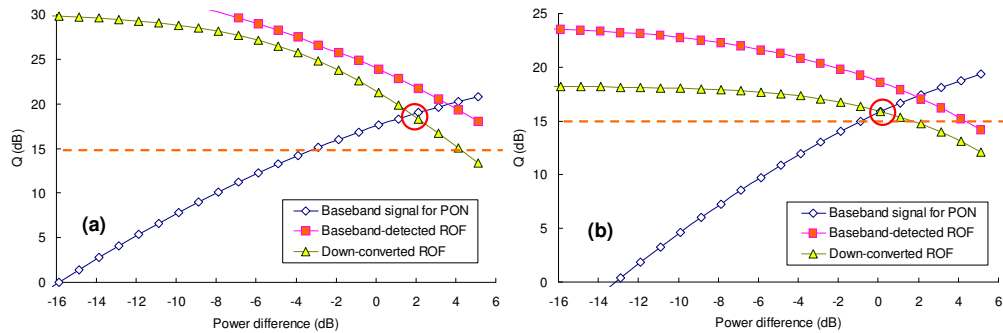


Fig. 7. Stimulated Q-value of the signals against power differences between the baseband NRZ and the ROF signals at (a) B2B and (b) after 60km SMF.

Figures 7(a) and 7(b) shows the simulated Q-value of different signals against the power difference,  $\Delta P$  ( $\Delta P = \text{power of baseband NRZ} - \text{power of ROF}$ ) at back-to-back (B2B) and after 60 km SMF transmission. When the power of the baseband NRZ increases (i.e.  $\Delta P$  increases), its performance will increase; however, it will produce higher crosstalk to the ROF signal. Hence there is a trade-off between them. At B2B, the optimum performance of both baseband NRZ and down-converted ROF signal is at  $\Delta P = 2$  dB. Since the ROF has a much broader spectrum than the baseband NRZ signal, it is more influenced by the fiber chromatic dispersion. Hence, after 60 km SMF transmission, the optimum power difference decreases to 0 dB. This implies that the launching power of the baseband NRZ signal should decrease accordingly to maintain the performance of the ROF signal, as shown in Fig. 7(b).

It is worth to mention that this scheme can be applied for much higher bit-rate. We then discuss the scalability of the system for bit-rate of 30 Gb/s using simulation. And 16.67 ps DI is used in this case. In the simulation, 30 Gb/s baseband NRZ signal is orthogonally wavelength division multiplexed with the 60 GHz ROF signal (carrying 30 Gb/s data) at different  $\Delta P$ . Signal at 60 GHz band is highly desirable for the future home network since it is licence-free [16]. The signals were transmitted through 20 km feeder SMF, which is fully dispersion compensated by using dispersion compensating fiber. Different lengths of SMF (dispersion parameter = 17 ps/nm/km) were included to evaluate the dispersion tolerance of the 60 GHz system at different drop fiber lengths. Figure 8 shows the simulated Q-value of the 60 GHz system. We can observe the opposite behaviour of the performances of the baseband and down-converted signals when  $\Delta P$  increases, and this has been explain in last paragraph. And the dispersion tolerance of the 60 GHz is more than 1 km of additional SMF, which could be long enough for the drop fiber.

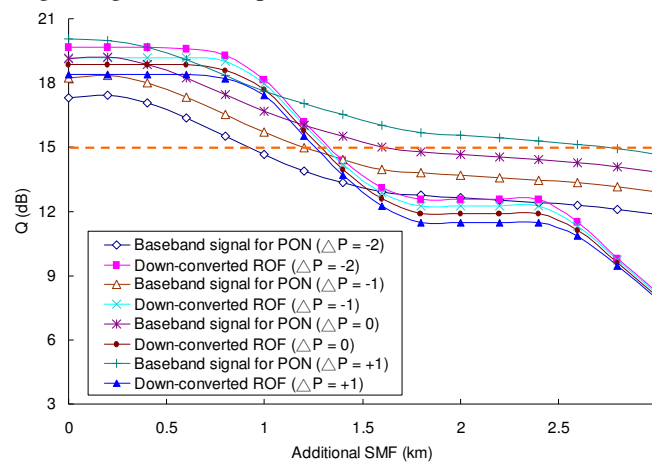


Fig. 8. Stimulated Q-value of the signals with different additional lengths of SMF.

## 5. Conclusion

We proposed and demonstrated a convergent optical wired and wireless LR access network using high spectral efficient orthogonal WDM to optically multiplex both baseband and ROF signal. Error-free de-multiplexing and down-conversion can be achieved for all the signals after 60 km fiber transmission. The operation principle was discussed; and the time-delays and power differences for achieving the optimum signal performances were also characterized. The scalability of the system for higher bit-rate at 60 GHz was also simulated and discussed.

## Acknowledgments

This work was financially supported by the National Science Council, Taiwan, R.O.C., under Contract NSC- 100-2221-E-009-088-MY3 and NSC-98-2221-E-009-017-MY3.